The size change of ferromagnetic domains induced by the effect of cation disorder in oxide perovskites

2004 J. Phys.: Condens. Matter 16 1631

(http://iopscience.iop.org/0953-8984/16/9/011)

INSTITUTE OF PHYSICS PUBLISHING JOURNAL OF PHYSICS: CONDENSED MATTER

J. Phys.: Condens. Matter **16** (2004) 1631–1638 PII: S0953-8984(04)70862-0

The size change of ferromagnetic domains induced by the effect of cation disorder in oxide perovskites

Shengming Zhou[1], Jun Xu[1], Guangjun Zhao[1], Shuzhi Li[1], Hongjun Li[1], Yin Hang[1], JingRong Cheng[2] and Yuheng Zhang[3]

[1] Shanghai Institute of Optics and Fine Mechanics, Chinese Academy of Sciences, Shanghai 201800, People's Republic of China
[2] Department of Physics, Anhui University, Hefei 230039, People's Republic of China
[3] Structure Research Laboratory, University of Science and Technology of China, Hefei 230026, People's Republic of China

Received 20 October 2003
Published 20 February 2004
Online at stacks.iop.org/JPhysCM/16/1631 (DOI: 10.1088/0953-8984/16/9/011)

Abstract

A-site cation disorder effects on the structural, electrical transport and magnetic properties have been studied in the $Nd_{0.7}(Ca, Sr, Ba)_{0.3}MnO_3$ series with a fixed A-site mean radius $\langle r_A \rangle = 1.21$ Å by resistivity, dc susceptibility, infrared spectra and thermopower measurements. The disparity of transition temperature obtained from resistivity, magnetization and thermopower increases with increasing amounts of A-site cation disorder quantified by the size variance σ^2. The insulator-like ferromagnetic behaviour and the sign change of thermopower induced by σ^2 have been observed below the Curie temperature T_C. As σ^2 increases, the size of the ferromagnetic domains decreases, and the carriers seem to be trapped strongly in the interfaces between ferromagnetic domains; such behaviours may help to understand the insulator-like ferromagnetic state induced by σ^2 below T_C.

1. Introduction

The colossal magnetoresistance (CMR) materials $L_{1-x}M_xMnO_3$ (L = rare earth; M = alkaline earth) have attracted much interest due to their potential technological applications and the fascinating physics involved [1]. The metal–insulator (M–I) and the paramagnetic (PM)–ferromagnetic (FM) transition temperatures are very close to each other and the CMR response is produced around Curie temperature T_C. This phenomenon was initially explained in terms of a double-exchange mechanism, in which FM coupling between localized Mn t_{2g} spins is mediated by itinerant e_g electrons [2]. However, this mechanism is insufficient to account for the observed transport behaviours in these mixed-valent manganites, and accumulating theoretical and experimental evidence [3–7] indicates that the extra physics associated with electron–lattice coupling, such as strong Jahn–Teller-type coupling [6] and nonmagnetic randomness [7], appears to play an important role.

Table 1. The cation-size variance σ^2, the residual resistivity ρ_0 measured at 15 K, the metal–insulator transition temperature T_m, the Curie temperature T_C and the unit-cell volume V_c measured at room temperature for a series of $Nd_{0.7}(Ca, Sr, Ba)_{0.3}MnO_3$ perovskites with constant $\langle r_A \rangle = 1.21$ Å.

	Sample	σ^2 (Å^2)	ρ_0 (Ω cm)	T_m (K)	T_C (K)	V_c (Å^3)
1	$Nd_{0.7}Sr_{0.3}MnO_3$	0.0045	0.006	211	215	230.420(5)
2	$Nd_{0.7}Ca_{0.033}Sr_{0.24}Ba_{0.027}MnO_3$	0.0058	0.02	182	185	230.525(3)
3	$Nd_{0.7}Ca_{0.066}Sr_{0.18}Ba_{0.054}MnO_3$	0.0070	1.07	152	156	230.625(3)
4	$Nd_{0.7}Ca_{0.099}Sr_{0.12}Ba_{0.081}MnO_3$	0.0083	13.9	119	132	230.719(4)
5	$Nd_{0.7}Ca_{0.132}Sr_{0.06}Ba_{0.108}MnO_3$	0.0096	2100	84	114	230.796(5)
6	$Nd_{0.7}Ca_{0.165}Ba_{0.135}MnO_3$	0.0108	—	—	102	230.860(3)

A-site cation disorder was extensively studied recently [8–12]. Rodriguez-Martinez and Attfield [8, 9] employed the size variance of the A-cation radius distribution, $\sigma^2 = \langle r_A^2 \rangle - \langle r_A \rangle^2$, to quantify the A-site cation disorder. It has been observed that the M–I transition temperature T_m shows a strong linear dependence upon σ [8, 10, 11]. A-site cation disorder can produce random oxygen displacements and, as a consequence, an enhanced local distortion of the MnO_6 octahedron. Such distortions can slow down the e_g electrons that mediate the FM interaction between Mn ions and thus influence the magnetic and transport processes in the manganites. However, it is still difficult to understand the fact that the residual resistivity increases dramatically and meanwhile the saturation magnetization remains almost unchanged with increasing σ^2 [9, 11]. In order to further understand such observed phenomena, we prepared a series of six $Nd_{0.7}(Ca, Sr, Ba)_{0.3}MnO_3$ samples (table 1) in which σ^2 is systematically varied by use of different compositions of Ca, Sr and Ba in this paper. Our samples are designed to have a fixed rare-earth element (Nd), a fixed doping level ($x = 0.3$) and a fixed mean A-site radius ($\langle r_A \rangle = 1.21$ Å is calculated by the use of ninefold coordination for A cations [13]) in order to ensure that the observed changes are mainly caused by A-site cation disorder. We performed the measurements of XRD, resistivity, dc magnetization, infrared (IR) spectrum and thermopower on $Nd_{0.7}(Ca, Sr, Ba)_{0.3}MnO_3$ samples, and present possible explanations for the observed results.

2. Experiment

The samples were prepared from stoichiometric amounts of Nd_2O_3, MnO_2, $CaCO_3$, $SrCO_3$ and $BaCO_3$ by solid state reaction under identical conditions. After pre-sintering with three intermediate grindings in air at 1000–1200 °C for three days, the mixtures were then pressed into discs and sintered at 1420 °C for 16 h. In order to minimize micro-inhomogeneity, the hard sintered discs were broken into pieces, reground to fine powder and again pressed into discs. The final sintering was carried out in air at 1440 °C for 12 h. X-ray powder diffraction (XRD) analyses were performed using an MXP18AHF x-ray diffractometer. Structural parameters were refined by the Rietveld method and XRD patterns indicate that the obtained samples are clearly of single phase with *Pnma* space group. The room temperature unit-cell volume (see table 1) does not change significantly with σ^2, as might be expected for samples with a fixed $\langle r_A \rangle$ and doping level. The magnetizations of bulk samples were recorded using a Lake Shore M9300 vibrating sample magnetometer. The measurements of IR transmission spectra (Nicolet 700) are carried out with powder samples in which KBr is used as a carrier. The thermoelectric power measurements were performed in a cryostat working from 300 K down to liquid nitrogen temperature. The SEM micrographs were obtained using a JEOL

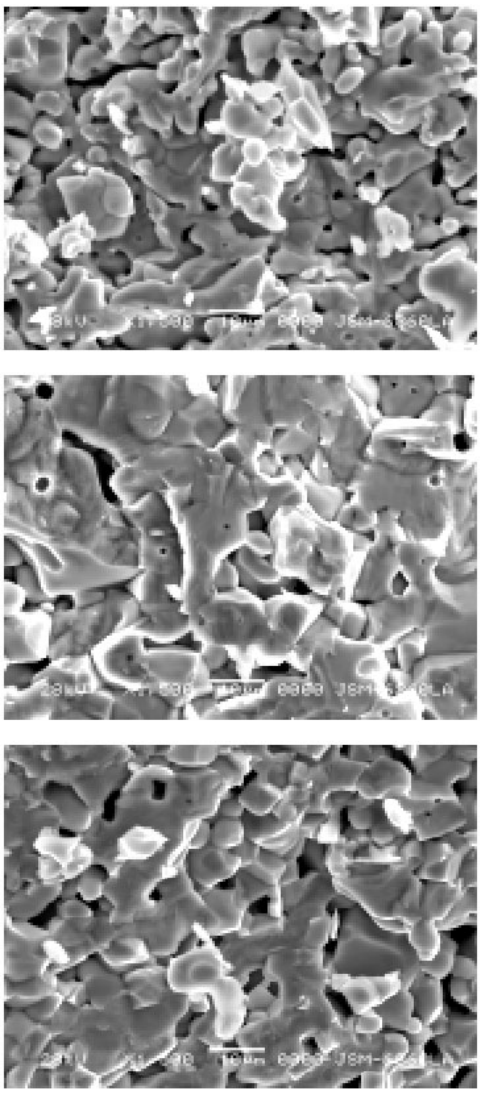

Figure 1. The SEM images for the samples 1, 4 and 6 in sequence.

JSM-6360LA microscope with an EDS attachment. Resistivity was measured by the standard four-probe technique.

3. Experimental results

The SEM images as shown in figure 1 are corresponding to samples 1, 4 and 6 (from top to bottom), respectively. In this series of six $Nd_{0.7}(Ca, Sr, Ba)_{0.3}MnO_3$ samples, the micro-particles exhibit various shapes and the particle size varies widely with average size of about 10 μm. But the particle aspects in shape and size between different samples are quite similar, and such a SEM result is rational because these six samples were sintered under the same conditions.

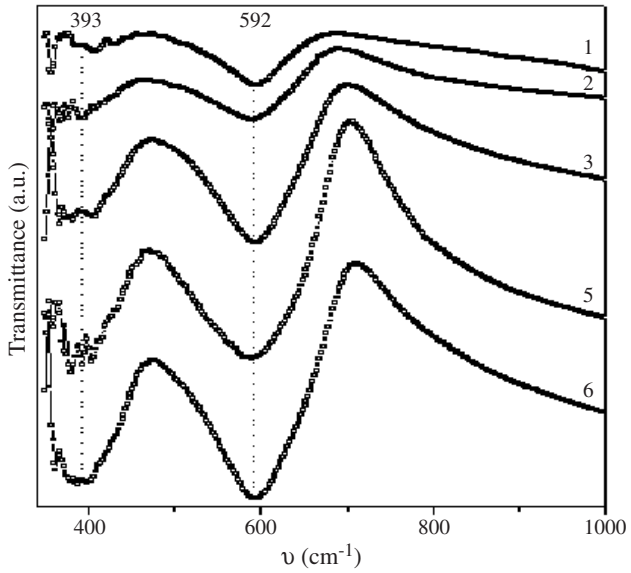

Figure 2. IR transmittance spectra at room temperature for $Nd_{0.7}(Ca, Sr, Ba)_{0.3}MnO_3$ with $\sigma^2 = 0.0045, 0.0058, 0.0070, 0.0096$ and 0.0108 Å^2, respectively. The curves are numbered according to table 1.

A-site cation disorder results mainly in random displacements of oxygen atoms from their average crystallographic positions [8, 9]. Direct evidence for this can be obtained from IR spectra which are sensitive to local lattice distortions [4, 14]. Figure 2 depicts the observed IR spectra of the five mixed oxides with $\sigma^2 = 0.0045, 0.0058, 0.0070, 0.0096$ and 0.0108 Å^2, respectively. The negative peaks around $\upsilon_3 = 592\ \mathrm{cm}^{-1}$ are assigned to the stretching vibration mode of the MnO_6 octahedron in which the Mn–O bond distance is modulated, and the negative peaks around $\upsilon_4 = 393\ \mathrm{cm}^{-1}$ to the bending vibration in which the Mn–O–Mn bond angle is modulated [4, 14]. As seen in figure 2, the bending vibration becomes more prominent with increasing σ^2; this reflects directly the fact that the symmetry of the local MnO_6 octahedra reduces with increasing σ^2 due to random displacements of oxide ions.

The temperature dependence of resistivity at zero field for the six samples, which are numbered in order of increasing σ^2, is shown in figure 3. Samples 1–5 exhibit a clear transition from insulator to metallic-like behaviour. Increasing σ^2 causes a decrease in T_m and an increase in the magnitude of resistivity. For the sample with $\sigma^2 = 0.0108$ Å^2, measurements were carried out down to 50 K and no metal transition was observed; however, the sample is ferromagnetic at low temperatures with $T_C = 102$ K (see table 1) according to the magnetization measurements. Here, the Curie temperature T_C is defined as the temperature corresponding to the inflection point in the magnetization curve.

Thermopower $S(T)$ is expected to be very sensitive to local moments and it can monitor the FM transition more sensitively, because it is less affected by the interfaces of the grains than resistivity and magnetization [15]. As shown in figure 4, each sample shows a positive enhancement of $S(T)$ as the sample was cooled from room temperature, and $S(T)$ has a tendency to collapse as T_C is approached from high temperatures. When $\sigma^2 \geqslant 0.0096$ Å^2, thermopower for samples 5 and 6 becomes unmeasurable at temperatures below about 120 K, where most of the carriers have become trapped. It is well known that the short range ferromagnetic correlations exist far above T_C in such manganese oxides [5]. The

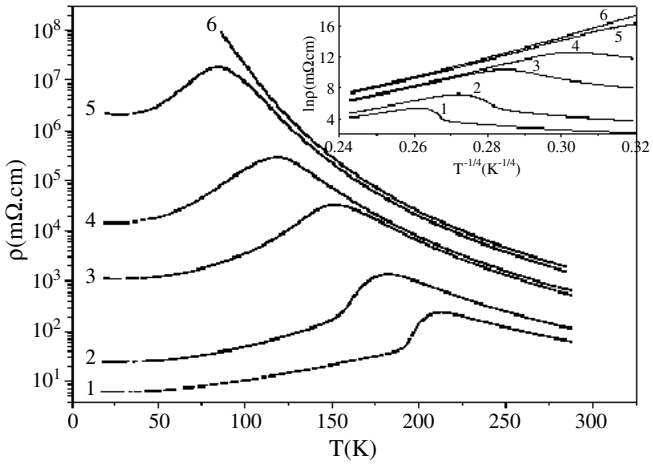

Figure 3. Temperature dependence of resistivity for $Nd_{0.7}(Ca, Sr, Ba)_{0.3}MnO_3$ with different variances σ^2. The inset shows $\ln(\rho)$ versus $T^{-1/4}$ for the corresponding samples.

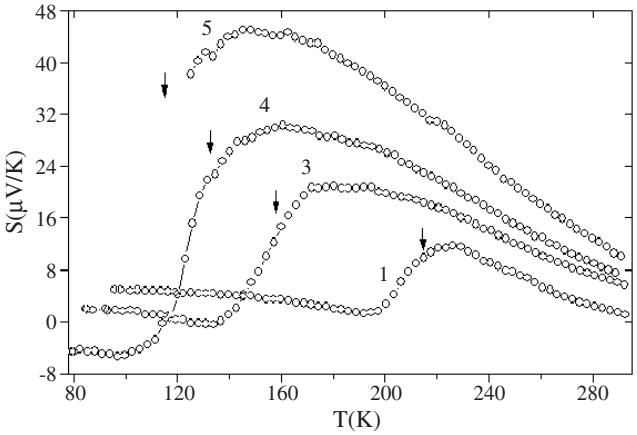

Figure 4. The temperature dependence of thermopower for $Nd_{0.7}(Ca, Sr, Ba)_{0.3}MnO_3$. The arrow indicates T_C.

collapsing tendency of thermpower implies that the strength of the ferromagnetic correlations is significantly enhanced when the temperature approaches T_C.

Figure 5 shows the σ^2 dependence of T_m, T_C and T_S (the temperature corresponding to the peak value of thermopower) for the $Nd_{0.7}(Ca, Sr, Ba)_{0.3}MnO_3$ series. T_m shows a strong linear dependence on σ^2, and gives the slope $dT_m/d\sigma^2 = -24\,907 \pm 472$ K Å^{-2} in the present samples. So far, the experiment data have shown that $|dT_m/d\sigma^2|$ increases with decreasing $\langle r_A \rangle$ in the $L_{0.7}M_{0.3}MnO_3$ system [8, 11]. For example, the absolute value of the slope is about 17 400, 20 600 and 24 907 K Å^{-2} for $\langle r_A \rangle = 1.26$, 1.23 and 1.21 Å, respectively. This reflects the fact that the effect of A-site cation disorder on T_m becomes strong when $\langle r_A \rangle$ decreases from the ideal radius $r_A^0 = 1.30$ Å (equivalent to a perovskite tolerance factor of 1.0). This can help to understand why the ferromagnetic insulator behaviour induced by σ^2 was observed in the present sample with $\langle r_A \rangle = 1.21$ Å rather than in the ones with $\langle r_A \rangle = 1.26$ and 1.23 Å [8, 11]. In figure 5, the most significant phenomenon is that T_C and T_S gradually deviate from linearity

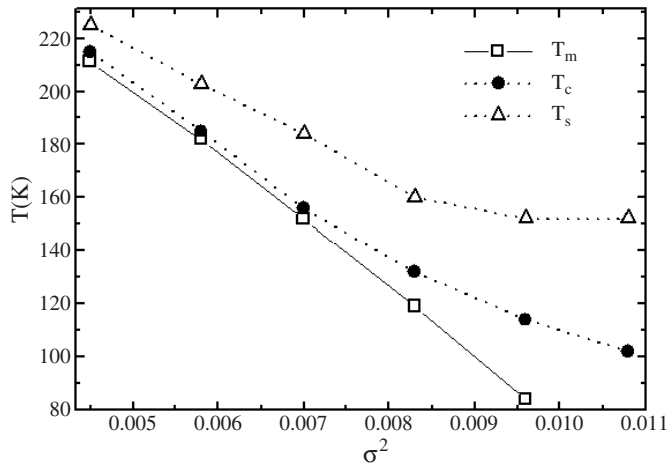

Figure 5. The metal–insulator transition temperature T_m, Curie temperature T_C and the peak temperature T_S of thermopower versus σ^2.

as σ^2 increases and that the relation $T_S > T_C > T_m$ can be obtained for each sample. The implications of these facts will be discussed in the next section.

4. Discussion

The internal phonon mode of v_3 is sensitive to the Mn–O bond length, and related to Jahn–Teller distortions. According to the IR results, no frequency shifts of the v_3 mode were observed with σ^2; this implies that the force constant of the Mn–O bond is not significantly affected by σ^2. However, the internal phonon mode of v_4, which is sensitive to a change in the Mn–O–Mn bond angle, varies obviously with σ^2. From the difference of IR spectra between samples 1 and 6, it can be obtained that the v_4 mode is significantly activated in the sample with larger σ^2. Therefore, A-cation disorder results mainly in random rotations of the local MnO_6 octahedra which can be viewed as the random impurity potential in the lattice. The conduction carriers are strongly localized due to such local lattice distortions caused by random rotations of MnO_6 octahedra and the resistivity is governed mainly by the variable range hopping above T_m in the samples with large σ^2 (see the inset in figure 3). The local distortions increase and the number of itinerant e_g electrons decreases with increasing σ^2; consequently, the size of ferromagnetic clusters, which are built depending on hopping e_g electrons, may tend to decrease. As a result, the FM transition temperature decreases with increasing σ^2.

However, the enormously large residual resistivity and the insulator-like ferromagnetic state cannot be explained only by the electron-localizing effects due to distortions of the MnO_6 octahedra. In our samples, A-site divalent cations with large size disparities may lead to a local micro-inhomogeneity in A-site ion distribution of bivalence and trivalence, so that a local variation of Mn oxidation state can be caused. This kind of inhomogeneity increases and gives rise to an increasing broadening of the PM–FM transition with increasing σ^2, which can be clearly seen in $S(T)$ curves around T_C (see figures 4). Therefore, the neighbouring FM regions are actually separated by the remaining PM interfaces in the FM state. As temperature further decreases, the remaining PM compositions decrease and may finally vanish, leaving FM domains with different magnetization directions in the grains. It can be expected that the FM domains may be subject to splitting and domain–domain interactions may become weaker as temperature rises towards T_C due to the increasing amounts of PM compositions.

In fact, similar magnetic domain behaviours have been observed directly by a magnetic force microscope in $La_{0.65}Ca_{0.35}MnO_3$ thin film [16]. Therefore, the rapid increase of the residual resistivity should be related to the decreasing size of FM domains with increasing σ^2. The e_g electrons may be trapped strongly in the interfaces between FM domains.

The decreasing size of FM domains with increasing σ^2 can lead to increasing magnetic fluctuations in the FM state. Such an effect can be reflected by the thermopower. It has been successfully demonstrated in $La_{0.75}Sr_{0.25}MnO_3$ and $La_{2/3}Ca_{1/3}MnO_3$ below T_C that increasing the degree of spin disorder can decrease the thermopower [17, 18]. In figure 4, the thermopower is reduced and a sign change is caused below T_C due to increasing σ^2; this implies that magnetic fluctuations increase with increasing σ^2 around T_C.

When samples are cooled to T_C, ferromagnetic correlations become strong and consequently the thermopower starts to collapse (see figure 4). Therefore, S is the most sensitive technique to detect the FM transition as compared with resistivity and magnetization. As the sample is further cooled, the size of ferromagnetic clusters sharply increases, and an upturn can be seen in the $M(T)$ curve. In the case of larger σ^2, though the FM state has occurred and e_g electrons can hop freely within FM domains, the carriers are still strongly trapped in the interfaces between FM domains due to the smaller size of domains; therefore, the M–I transition has not occurred until the temperature is further lowered below T_C. Such a mechanism is responsible for the disparity of T_m, T_C and T_S, and thus the relation of $T_S > T_C > T_m$ can be observed in the present samples (see figure 5). The disparity of T_m, T_C and T_S clearly suggests that the size of FM domains in grains becomes smaller with increasing σ^2. In addition, it is well known that the disparity between T_m and T_C will increase as the crystalline grains become smaller in polycrystalline samples [19]. The observed disparity between T_m and T_C in the present work is due to the size decrease of FM domains in grains, however not due to the size decrease of grains, because the average grain size of the samples with different σ^2 is almost the same as shown in figure 1.

5. Conclusions

In summary, we studied the A-site cation disorder effects in polycrystalline $Nd_{0.7}(Ca, Sr, Ba)_{0.3}MnO_3$ with a fixed $\langle r_A \rangle = 1.21$ Å by means of a combination of XRD, resistivity, dc magnetization, IR spectra and thermopower measurements. The disparity of transition temperature obtained from resistivity, magnetization and thermopower increases with increasing σ^2. The insulator-like ferromagnetic behaviour and the sign change of thermopower induced by σ^2 have been observed below T_C. IR spectra show that A-site cation disorder causes random rotations of local MnO_6 octahedra. Increasing σ^2 may weaken FM interactions and decrease the size of FM domains. The carriers are strongly localized in the interfaces between the FM domains and this may be responsible for the insulator-like ferromagnetic state in the sample with large σ^2.

Acknowledgments

This work was supported by the Fund for Scientific Research of SIOM(X030805). One of the authors was supported by a Grant-in-Aid (No. 00047208) from the Natural Scientific Research Fund of Anhui Province.

References

[1] Millis A J 1998 *Nature* **392** 147
[2] Zener C 1951 *Phys. Rev.* **82** 403

[3] Uehara M, Mori S, Chen C H and Cheong S-W 1999 *Nature* **399** 560
[4] Kim K H, Gu J Y, Choi H S, Park G W and Noh T W 1996 *Phys. Rev. Lett.* **77** 1877
[5] De Teresa J M, Ibarra M R, Algarabel P A, Ritter C, Marguina C, Blasco J, García J, del Moral A and Arnold Z 1997 *Nature* **386** 256
[6] Millis A J, Littlewood P B and Shraiman B I 1995 *Phys. Rev. Lett.* **74** 5144
[7] Sheng L, Xing D Y, Sheng D N and Ting C S 1997 *Phys. Rev.* B **56** R7053
[8] Rodriguez-Martinez L M and Attfield J P 1996 *Phys. Rev.* B **54** R15622
[9] Rodriguez-Martinez L M and Attfield J P 1998 *Phys. Rev.* B **58** 2426
[10] Damay F, Martin C, Maignan A and Raveau B 1997 *J. Appl. Phys.* **82** 6181
[11] Rodriguez-Martinez L M, Ehrenberg H and Attfield J P 1999 *J. Solid State Chem.* **148** 20
[12] Vanitha P V, Santhosh P N, Singh R S, Rao C N R and Attfield J P 1999 *Phys. Rev.* B **59** 13539
[13] Shannon R D 1976 *Acta Crystallogr.* A **32** 751
[14] Zhou S M, Zhou G E and Zhang Y H 1999 *Japan. J. Appl. Phys.* **38** 5075
[15] Archibald W, Zhou J-S and Goodenough J B 1996 *Phys. Rev.* B **53** 14445
[16] Lu Q Y, Chen C C and Lozanne A D 1997 *Science* **276** 2006
[17] Asamitsu A, Moritomo Y and Tokura Y 1996 *Phys. Rev.* B **53** R2952
[18] Jaime M, Salamon M B, Rubinstein M, Treece R E, Horwitz J S and Chrisey D B 1996 *Phys. Rev.* B **54** 11914
[19] Zheng L, Li K B and Zhang Y H 1998 *Phys. Rev.* B **58** 8613